## Electronic Supplementary Information (ESI)

for DOI: 10.1039/x0xx00000x

# An EPR Investigation of Defect Structure and Electron Transfer Mechanism in Mixed-Conductive $LiBO_2$-$V_2O_5$ Glasses

Jacob N. Spencer,*[a] Andrea Folli,[a] Hong Ren[b] and Damien M. Murphy[a]

[a.] *School of Chemistry, Cardiff University, Main Building, Park Place, Cardiff CF10 3AT, UK*
[b.] *Johnson Matthey Technology Centre, Blounts Court Road, Sonning Common, Reading, Berkshire RG4 9NH, UK*

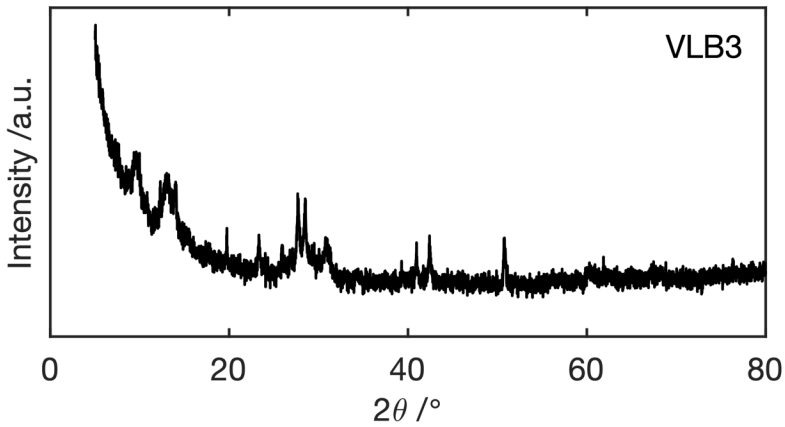


**Figure S1**: Experimental X-ray diffraction pattern of VLB3 exhibiting very low degree of crystallinity, evidence of the amorphous character of the material.

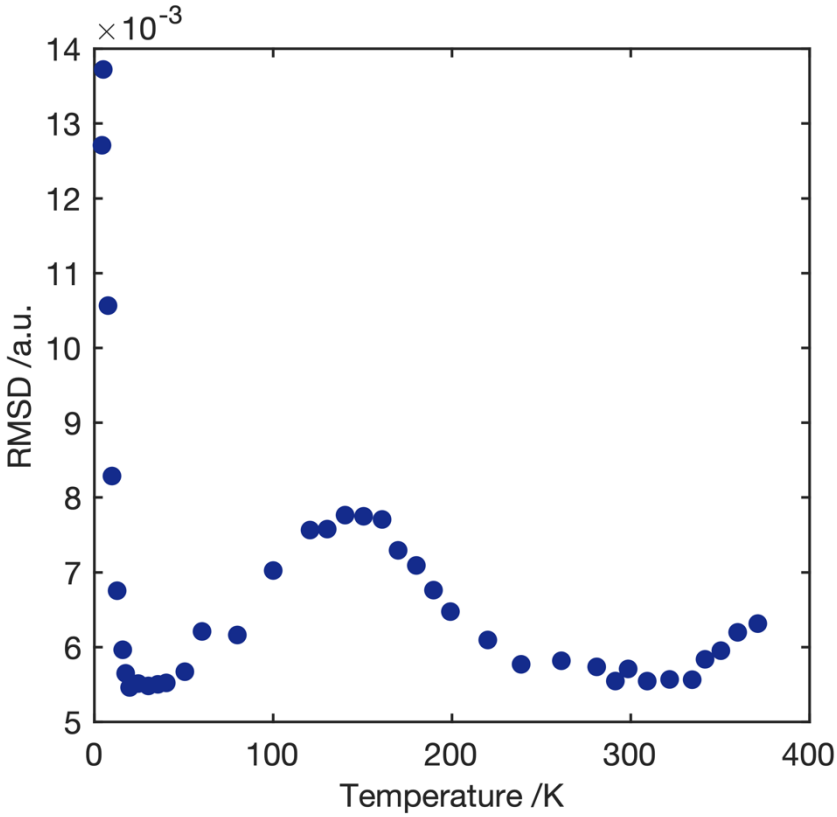


**Figure S2:** Calculated root mean square deviation for variable temperature fitting of VLB3, indicating goodness of fit and relative error.

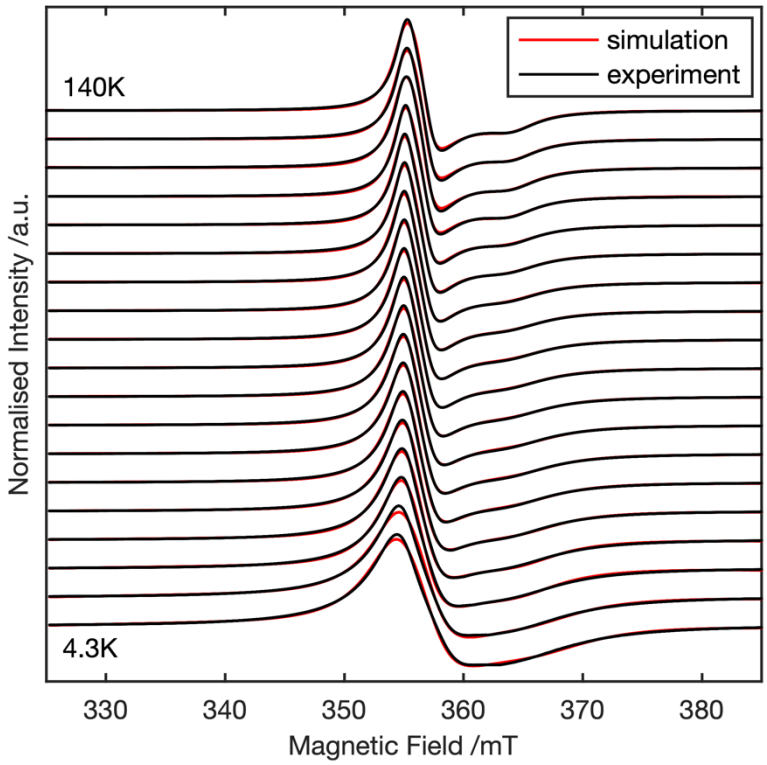


**Figure S3:** Fitting of VLB3 variable temperature spectra between *T* = 4.3 K to 100 K.

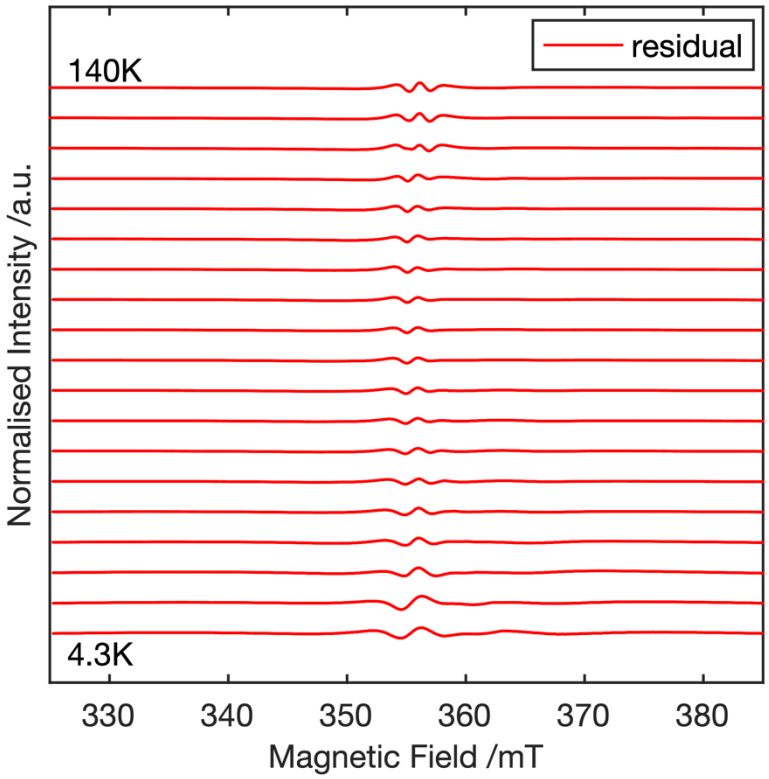


**Figure S4**: Calculated residuals of VLB3 variable temperature spectra between *T* = 4.3 K to 100 K.

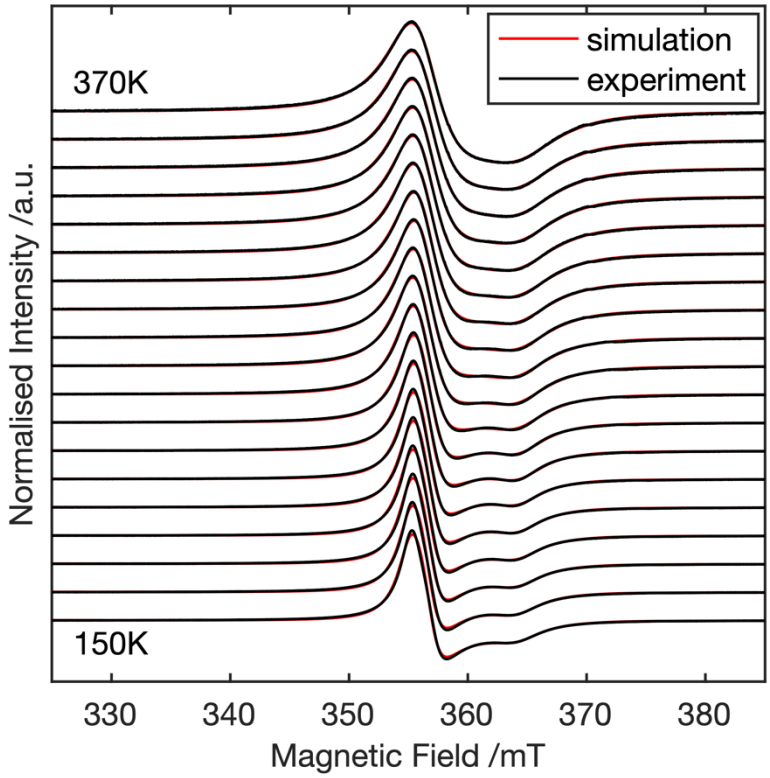


**Figure S5:** Fitting of VLB3 variable temperature spectra between *T* = 120 K to 370 K.

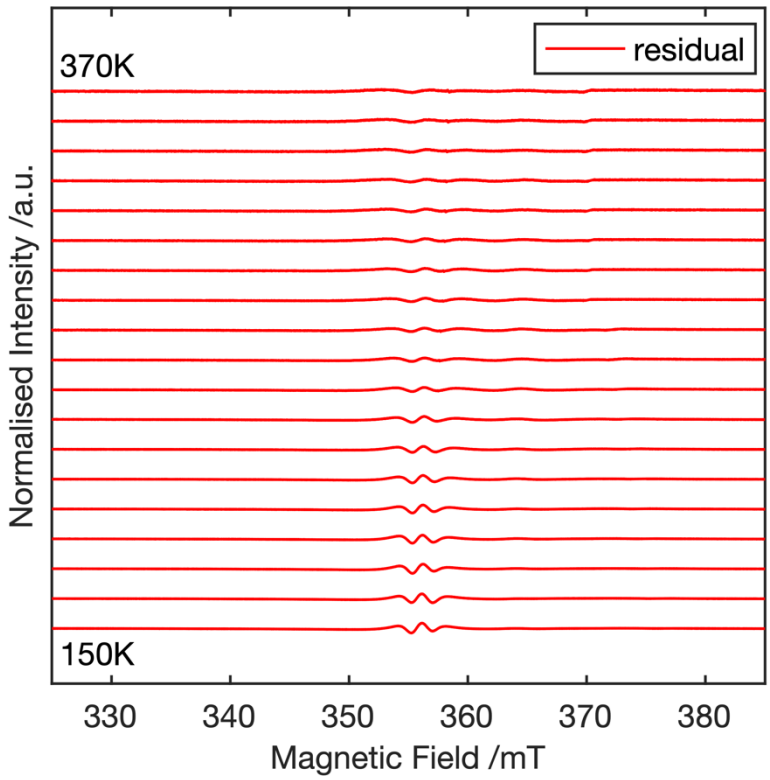


**Figure S6:** Calculated residuals of VLB3 variable temperature spectra between *T* = 120 K to 370 K.

**Simulation details for the variable temperature line width modelling (Figures 3, 4, 5 and 6)**

The anisotropic, Lorentzian line width for the $g_3$ component was calculated as the explicit superposition of individual Lorentzian lines of homogeneous linewidth ($\Delta B_{pp}$ as for $g_{1,2}$) which were summed and weighted using a normalised Lorentzian function of the form:

$$f_L(x) = \frac{2}{\pi\sqrt{3}}\frac{1}{\Gamma}\left[1+\frac{4}{3}\left(\frac{x-x_0}{\Gamma}\right)^2\right]^{-1}$$

where $x_0$ is the centre of the resonance and $\Gamma$ is the distance between the inflection points. The explicit calculation of the pure Lorentzian anisotropic line width was sufficient to accurately reproduce the line shape observed for VLB3.

**Table S1:** Simulation parameters obtained by least-squares fitting from the variable temperature study. The value of $\boldsymbol{\lambda}$ was fixed for the two temperature ranges reported after variation in the initial fitting routine. The reported *g*-components and line widths were obtained by a 2-step least-squares fitting routine, where the fitted minimum from the previous temperature were used as a starting point for the next fitting routine, and the *g* components (*blue*) and line widths (*orange*) were incremented in turn (and the other parameters were fixed for the routine step).

| $T$ /K | $g_1$ | $g_2$ | $g_3$ | $\Delta B_{pp}(T)$: $g_{1,2}$/mT | $\Delta B_{pp}(T)$: $g_3$/mT | $\lambda$ | r.m.s.d. |
|---|---|---|---|---|---|---|---|
| 4.3 | 1.9315 | 1.9956 | 1.9798 | 3.567 | 7.760 | -0.336 | 0.0127 |
| 5.0 | 1.9346 | 1.9944 | 1.9802 | 3.368 | 7.479 | -0.336 | 0.0137 |
| 7.6 | 1.9396 | 1.9934 | 1.9832 | 2.825 | 6.092 | -0.336 | 0.0106 |
| 9.8 | 1.9396 | 1.9934 | 1.9835 | 2.575 | 5.850 | -0.336 | 0.0083 |
| 12.7 | 1.9397 | 1.9930 | 1.9838 | 2.392 | 6.071 | -0.336 | 0.0068 |
| 15.9 | 1.9405 | 1.9931 | 1.9836 | 2.171 | 5.961 | -0.336 | 0.0060 |
| 17.5 | 1.9408 | 1.9931 | 1.9836 | 2.061 | 5.830 | -0.336 | 0.0056 |
| 19.7 | 1.9409 | 1.9931 | 1.9835 | 1.994 | 5.805 | -0.336 | 0.0055 |
| 24.5 | 1.9421 | 1.9931 | 1.9835 | 1.880 | 5.572 | -0.336 | 0.0055 |
| 30.2 | 1.9429 | 1.9932 | 1.9833 | 1.740 | 5.297 | -0.336 | 0.0055 |
| 35.5 | 1.9429 | 1.9932 | 1.9833 | 1.679 | 5.213 | -0.336 | 0.0055 |
| 40.2 | 1.9434 | 1.9932 | 1.9833 | 1.631 | 4.985 | -0.336 | 0.0055 |
| 50.6 | 1.9444 | 1.9933 | 1.9834 | 1.568 | 4.816 | -0.336 | 0.0057 |
| 60.2 | 1.9442 | 1.9932 | 1.9834 | 1.516 | 4.439 | -0.336 | 0.0062 |
| 80.0 | 1.9442 | 1.9932 | 1.9834 | 1.470 | 4.223 | -0.336 | 0.0062 |
| 100.0 | 1.9443 | 1.9930 | 1.9834 | 1.472 | 3.737 | -0.336 | 0.0070 |
| 120.6 | 1.9444 | 1.9943 | 1.9849 | 1.587 | 3.552 | -0.083 | 0.0076 |
| 130.2 | 1.9442 | 1.9939 | 1.9849 | 1.574 | 3.441 | -0.083 | 0.0076 |
| 140.2 | 1.9443 | 1.9938 | 1.9848 | 1.557 | 3.288 | -0.083 | 0.0078 |
| 150.6 | 1.9438 | 1.9934 | 1.9847 | 1.587 | 3.265 | -0.083 | 0.0077 |
| 160.9 | 1.9440 | 1.9932 | 1.9848 | 1.581 | 3.105 | -0.083 | 0.0077 |
| 169.9 | 1.9436 | 1.9932 | 1.9843 | 1.585 | 3.102 | -0.083 | 0.0073 |
| 180.1 | 1.9437 | 1.9931 | 1.9845 | 1.647 | 3.080 | -0.083 | 0.0071 |

| | | | | | | | |
|---|---|---|---|---|---|---|---|
| 189.7 | 1.9436 | 1.9928 | 1.9843 | 1.694 | 3.028 | -0.083 | 0.0068 |
| 199.1 | 1.9435 | 1.9927 | 1.9843 | 1.750 | 3.054 | -0.083 | 0.0065 |
| 220.0 | 1.9433 | 1.9923 | 1.9843 | 1.942 | 3.103 | -0.083 | 0.0061 |
| 238.7 | 1.9431 | 1.9920 | 1.9842 | 2.121 | 3.239 | -0.083 | 0.0058 |
| 261.2 | 1.9437 | 1.9917 | 1.9842 | 2.339 | 3.682 | -0.083 | 0.0058 |
| 280.9 | 1.9436 | 1.9913 | 1.9845 | 2.590 | 3.889 | -0.083 | 0.0057 |
| 291.4 | 1.9436 | 1.9903 | 1.9850 | 2.757 | 4.020 | -0.083 | 0.0055 |
| 298.5 | 1.9431 | 1.9893 | 1.9851 | 2.862 | 4.113 | -0.083 | 0.0057 |
| 309.2 | 1.9431 | 1.9885 | 1.9858 | 3.012 | 4.266 | -0.083 | 0.0055 |
| 321.7 | 1.9431 | 1.9872 | 1.9872 | 3.175 | 4.413 | -0.083 | 0.0056 |
| 334.3 | 1.9430 | 1.9872 | 1.9872 | 3.307 | 4.541 | -0.083 | 0.0056 |
| 341.5 | 1.9429 | 1.9871 | 1.9873 | 3.397 | 4.640 | -0.083 | 0.0058 |
| 350.4 | 1.9429 | 1.9872 | 1.9872 | 3.515 | 4.782 | -0.083 | 0.0060 |
| 359.8 | 1.9429 | 1.9871 | 1.9872 | 3.636 | 4.884 | -0.083 | 0.0062 |
| 371.0 | 1.9428 | 1.9871 | 1.9872 | 3.778 | 5.040 | -0.083 | 0.0063 |

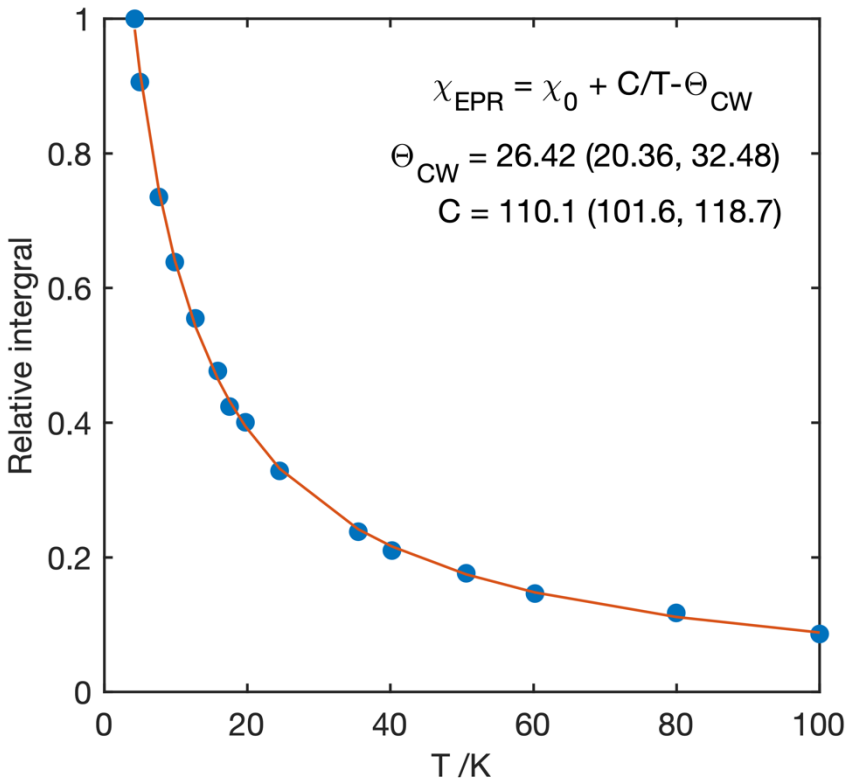


**Figure S7:** Calculated double integrated intensity of VLB3 across the entire signal at free spin.

**Simulation details for the variable frequency EPR study (Figures 7 and S8)**

Software commonly used for EPR simulation (such as Easyspin reported here) does not allow for the calculation of an anisotropic Lorentzian line width for highly anisotropic, spin-relaxation dominated broadening which was attributed to the VLB3 system. This anisotropic line width was therefore calculated explicitly for the system which was described in the ESI *vide* infra. The simulation of the $V_2O_5$ type site in VLB was performed using the following scheme:

$$V^{4+}\text{--------}O\text{---------}V^{4+}$$

Where $V^{4+}$ denotes the uncoupled paramagnetic states. As mentioned in the main text, inter-site disorder is effectively screened from the spectrum due to the magnitude of *J* with respect to the difference in Zeeman energies ($\Delta g\mu_B B$). The *g*-tensors of the uncoupled states (the two paramagnetic sites) were therefore assumed to be equivalent and collinear, since the strong exchange regime averages the difference in Zeeman energies between the disordered sites and orientational information (such as the relative orientation of the *g* principle axes) cannot be derived from powder EPR measurements.

The uncoupled states were correlated by *J* to form the coupled system. Finally, the anisotropic line width was calculated for the $g_3$ component as described above for the variable temperature study. The distribution (i.e. $\Gamma$) was corrected for field dependence by multiplying as the ratio of microwave frequencies (the line width does not broaden with increasing microwave frequency, as is the case for a distribution in *g*).

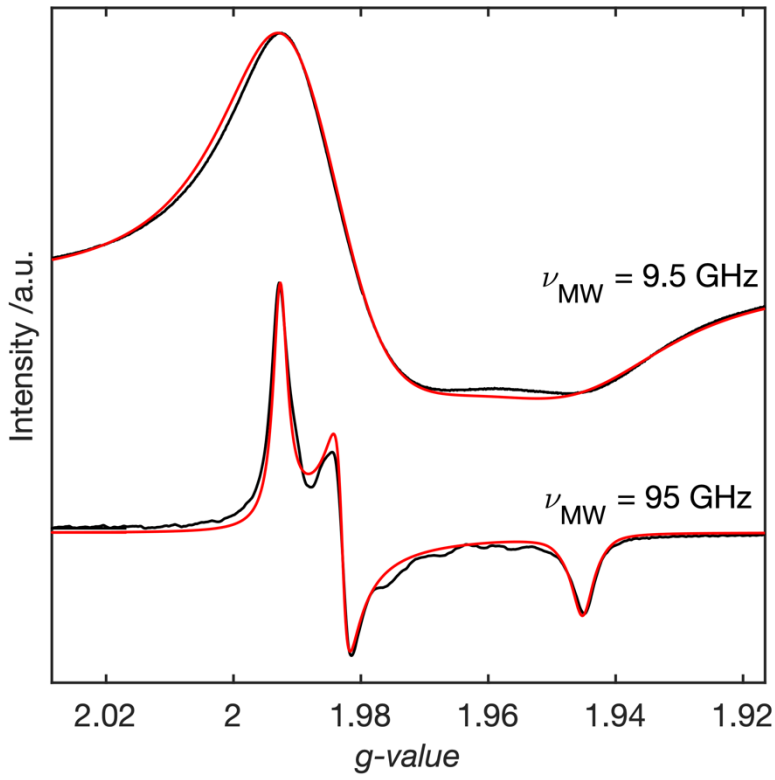


**Figure S8:** Simultaneous fitting of VLB3 sample at X-band and W-band frequencies and *T* = 300 K.